

# THE EVOLUTION OF STELLAR MASS IN THE NICMOS UDF AND THE CFHTLS DEEP FIELDS

Stephen Gwyn, F. D. A. Hartwick, Anudeep Kanwar, David Schade, Luc Simard  
*University of Victoria, Herzberg Institute of Astrophysics*

**Abstract.** We measure the build-up of the stellar mass of galaxies from  $z = 6$  to  $z = 1$ . Using 15 band multicolour imaging data in the NICMOS Ultra Deep Field we derive photometric redshifts and masses for 796 galaxies down to  $H_{AB} = 26.5$ . The derived evolution of the global stellar mass density of galaxies is consistent with previous star formation rate density measurements over the observed range of redshifts. Ongoing research in the CFHTLS Deep Fields confirms this result at lower redshifts. Further, if the sample is split by morphological type, a substantial increase is seen in the number of bulge dominated galaxies relative to disk-dominated galaxies since  $z = 1$ .

## 1 Introduction

For the last ten years, the Lilly-Madau diagram [1, 2, 3] has been central to the discussion of galaxy evolution. It shows that the star formation rate density (SFRD) increases with redshift to  $z \sim 1$  and decreases beyond that. In the last year, thanks to the Ultra Deep Field (UDF), several points have been added at the high-redshift end of the diagram [4, 5, 6, 7].

While the Lilly-Madau diagram is a useful tool for studying galaxy evolution, it is subject to some uncertainties, particularly at the high-redshift end. One source of uncertainty lies in identifying the high-redshift galaxies: the Balmer break may be confused with the Lyman break, putting spurious galaxies *in* the sample, and galaxies with heavy extinction may be left *out*. Extinction must also be considered when converting the UV flux into a SFR. Typically, a factor of 5 is used for the extinction correction, but the exact value is imperfectly known. For these reasons, it would be satisfying to have some corroboration of the SFR. This paper presents measurements of the global stellar mass density (GSMD) based on the NICMOS UDF.

It is also interesting to find out where and when exactly the mass builds up. Is it in disk galaxies or ellipticals? Red (older) galaxies or blue ones? High density or low density regions? This paper also presents preliminary measurements of stellar mass density split by morphological type in the CFHTLS Deep Fields.

## 2 NICMOS Ultra Deep Field: Global Mass Evolution to $z = 6$

The NICMOS UDF lies within the GOODS South region of the sky and has been imaged by a large number of telescopes at a variety of wavelengths. For this project four sources of imaging data for this field were considered:

- F110W band ( $J$ ) and F160W ( $H$ ) from NICMOS on HST.
- F435W ( $B$ ), F606W (somewhere between  $V$  and  $R$ ), F775W ( $I$ ) and F850LP ( $Z$ ).
- $JHK'$  imaging from ISAAC on VLT.
- $U'UBVRI$  from the ESO Imaging Survey.

The F160W image was used as a reference image. All the other images were resampled using SWarp<sup>1</sup> to match this image. SExtractor [8] was run in double-image mode on all the images in all the bands with the NICMOS F160W ( $H$ -band) image as the reference image. Variable elliptical apertures (SExtractor's MAG\_AUTO) were used.

Photometric redshifts were calculated for all the objects in the field. The usual template-fitting,  $\chi^2$  minimization method [9, 10] was used. The templates were based on the Coleman, Wu & Weedman (1980) [11] spectra. These are supplemented with the SB2 and SB3 spectra from Kinney et al. (1996) [12] as well as templates interpolated between the main 6 templates. The results are remarkably good. Comparison with the available secure spectroscopic redshifts show a  $\sigma_z = 0.06 \times (1 + z)$  spread with no catastrophic failures. If the less secure spectroscopic redshifts (including some AGNs) are included, this spread increases to  $\sigma_z = 0.12(1 + z)$ , with 2 catastrophic failures for 39 objects. The resampled images and catalogues are available on the web<sup>2</sup>.

<sup>1</sup>SWarp is available at: [http://terapix.iap.fr/rubrique.php?id\\_rubrique=49](http://terapix.iap.fr/rubrique.php?id_rubrique=49)

<sup>2</sup><http://orca.phys.uvic.ca/~gwyn/MMM/nicmos.html>

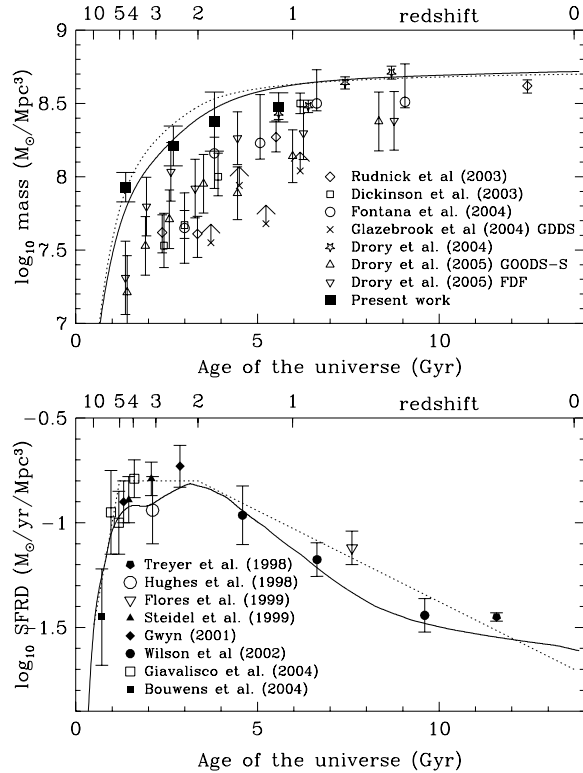


Figure 1: Stellar mass evolution. The bottom panel shows the SFR history of the universe. The points indicate measurements of the SFRD from the literature. The top panel shows the stellar mass evolution from this work along with data from the literature. The GDDS points are shown as lower limits. In both panels, the solid line shows the model of [16]. The dotted line is an arbitrary parameterization the SFR history (not a model) in the lower panel, and the integral of this parameterization in the upper panel. This figure is based on Figure 3 of Gwyn & Hartwick (2005).

We determined masses for each galaxy with a template fitting process similar to the photometric redshift method. The photometry for each galaxy is converted into an SED and compared to series of templates as before. In this case, the redshift of the templates being considered is held fixed during the  $\chi^2$  minimization.

Rather than the empirical Coleman, Wu & Weedman (1980)[11] and Kinney et al. (1996)[12] templates, a selection of the PEGASE 2.0[13] galaxy spectral evolution models were used as templates. The templates were redshifted as before and the IGM correction was applied.

The models span the full range of ages from  $t = 0$  to 14 Gyr. The metallicity was set to zero (no metals) at  $t = 0$  in the models. As each model evolves in time, the metallicity evolves self-consistently. We added extinction to the models using the reddening curve of Calzetti et al.[14]. The amount of extinction was varied from  $A(V) = 0$  to 1. The Kroupa (1993)[15] initial mass function (IMF) was used exclusively. The error on the derived masses is a function of apparent magnitude. It was estimated to be  $\sigma_{\text{mass}} = 0.1$  for  $H_{AB} < 25$  and  $\sigma_{\text{mass}} = 0.2$  for  $H_{AB} > 25$ .

The  $1/V_a$  method was used to compute mass functions in a series of redshift bins. The  $k$ -corrections were computed by interpolation using the best-fitting template from the photometric redshift procedure. To extrapolate beyond the observed range, Schechter functions were fit to the binned data. Integrating over these functions gives the total masses for each redshift bin.

To determine uncertainties on the global mass estimates, a Monte Carlo method was used. In the original catalogue of galaxies we added noise to the measured redshifts and masses according to the error estimates discussed above. Further, we simulated the effects of redshift error on the derived masses by noting the relative shift in luminosity distance caused by the redshift error, and applying the same shift to the mass. From this “noisy” catalogue we derived mass functions, integrated over fitted Schechter functions and computed total stellar masses. The RMS of the range of total stellar masses derived after 100 actualizations was used for the error bars in Figure 1.

Figure 1 shows the build up of stars in galaxies as function of time. The top panel shows the GSMD, while the bottom panel shows the SFR. The top panel can be thought of as  $M_{\star}(t)$ , while the bottom panel can be thought of as its derivative,  $dM_{\star}(t)/dt$ . This panel is the reverse of the Lilly-Madau diagram, with cosmic time instead of redshift on the horizontal axis. The bottom panel shows a number of measurements of the SFR from

the literature ([18, 19, 10, 20, 21, 22, 23]) from the compilation of Hartwick (2004)[16].

The upper panel shows our measurements of the GSMD as solid points, together with a number of measurements from the literature ([24, 25, 26, 27, 28]) as assorted open points. The corrections for the choice of IMF have been applied.

The solid line in both panels of Figure 1 come from Hartwick (2004) [16], who derived the global star formation history from observations of the local universe. Briefly, the model uses the distribution in metallicity of stars to derive  $dM_*/dZ$  (where  $Z$  is the metallicity) and the age-metallicity relationship for globular clusters to derive  $dZ/dt$  (where  $t$  is the age of the universe). Combining  $dM_*/dZ$  and  $dZ/dt$ , one obtains  $dM_*/dt \equiv$  SFR. This simple model does a very good job of explaining the star formation history of the universe, as shown by the agreement between it and the observations in the lower panel. Using this star formation history as an input to the PEGASE 2.0 software, we compute a model GSMD. The result is plotted in the upper panel. It is in excellent agreement with our GSMD measurements. Note that this agreement is not dependent on the details of the Hartwick model. Almost any description of the star formation history which agrees with the observed SFRs will, once integrated, produce good agreement with GSMD. This is illustrated by the dotted line in Figure 1. On the lower panel, this shows an arbitrary, three-segment ‘‘connect-the-dots’’ description of the star formation history. The three segments represent the rise of the SFR at  $z < 2$ , a plateau at  $2 > z > 5$  and the fall off at  $z > 5$ . In the upper panel the dotted line shows the results of integrating (again with PEGASE 2.0) this star formation history. Again, there is good agreement with our GSMD calculations.

### 3 CFHTLS Deep Fields: Mass Evolution by Morphological Type

This section presents results from ongoing research in the CFHT Legacy Survey. The CFHTLS Deep Fields are four pointings of the MegaCam wide field imager. Each field is 1 square degree and is imaged in the *ugriz* filters. The primary scientific goal of the Deep Fields is supernova cosmology. The fields are reimaged about once every two weeks and the supernovae are detected by comparing the current image with the previous image. The total exposure times are currently about 40 hours in the *i* band.

All the currently available exposures were astrometrically and photometrically calibrated using the *AstroGwyn* and *PhotoGwyn* packages and stacked using *Swarp*. The depth of the stacked images in AB magnitudes is roughly 26 for the *ugri* images and about 24 for the *z* image.

Photometric redshifts were calculated for every galaxy in the fields. A comparison with available spectroscopic redshifts from the DEEP2 galaxy survey shows a scatter of about  $\sigma = 0.08 \times (1 + z)$  with less than 1% catastrophic failures. The stacked images are available on the web to the Canadian and French communities<sup>3</sup>

The CFHTLS Deep Fields do not go as far out in redshift as the NICMOS UDF does. Also, the lack of infrared data means that care must be taken when measuring galaxy masses. However, the CFHTLS Deep Fields sample a far greater volume and consequently contain a much larger number of galaxies. The total sample can be split into a number of different subsamples to examine where stellar mass is building up. Ultimately, the sample will be split by colour (as a proxy for age) and by local environment (low density *vs.* high density) but for this work the sample was split by morphology.

Bulge-disk decomposition was done for every galaxy brighter than  $i_{AB} = 25$  using the *galfit* [29] package. The sample was split by bulge-to-total ratio. Galaxies with  $B/T < 0.5$  were assigned to the disk-dominated sample; those with  $B/T > 0.5$  to the bulge-dominated sample.

In the absence of infrared data, measurements of the stellar mass of galaxies must be made with caution. There is a danger that transitory starburst events will mask the underlying population. In the worst case scenario, as discussed by Rudnick et al.[24], this can lead to over-estimating the stellar mass by 70%. To avoid this, the galaxies in each bin (in  $B/T$  and redshift) were averaged together. For each redshift bin, luminosity functions were generated in 5 artificial bandpasses. These bandpasses correspond to the original 5 *ugriz* filters of the CFHTLS survey, but they are blue-shifted so that the artificial rest-frame bandpass is close to the observed filter. This minimizes the *k*-corrections. Integrating over these luminosity functions produces a coarse SED of the typical galaxy for that redshift and  $B/T$  bin. Fitting PEGASE2.0 model spectra to this SED yields a total stellar mass for the bin. By averaging in this way, the effects of any one starburst occurring in a particular galaxy are effectively masked. The only way the mass estimates can be biased is if most of the galaxies in a given bin have peculiar star-formation histories.

The results of this procedure are shown in Figure 2. The total mass evolution agrees well with the GSMD from Figure 1. The figure also shows that the mass density of bulge-dominated galaxies is increasing rapidly as a function of time (note that there are almost no bulge-dominated galaxies at  $z > 1$ ; this point is off the graph) while the mass in disk-dominated galaxies is dropping off slightly with increasing time/decreasing redshift. This result is similar to that of Bundy et al.[30]. They split their sample into ellipticals, disks and peculiars using traditional visual classification. They found that the mass in elliptical galaxies increased with time at the expense of disk and peculiar galaxies. Their differential evolution is not as extreme as the results presented here, probably because the  $B/T > 0.5$  cut used to select bulge-dominated galaxies also selected some earlier-type disk systems. The combination of the present work and Bundy et al.[30] argues that there is a strong trend

<sup>3</sup><http://orca.phys.uvic.ca/~gwyn/cfhtls/index.html>

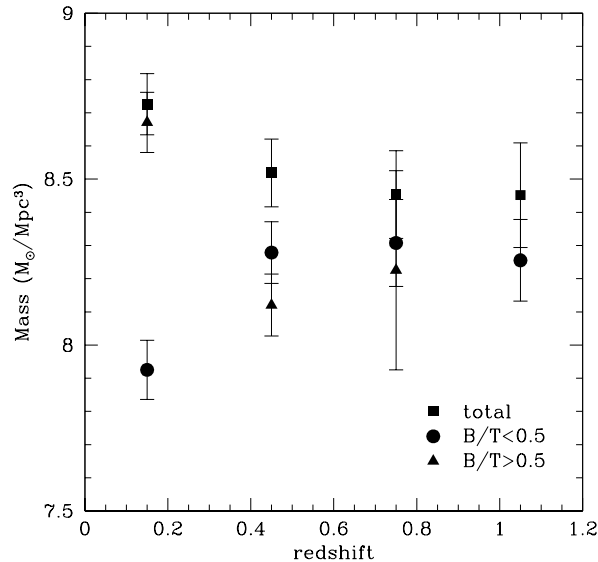


Figure 2: Stellar mass evolution for different morphological types: The squares show the total mass in stars as a function of redshift. The circles and triangles show the same, but for disk-dominated and bulge-dominated galaxies respectively.

toward more massive bulges in galaxies since  $z = 1$ , with a less extreme trend towards complete disruption of their disks.

## 4 Summary

- Work on the NICMOS UDF shows that the global stellar mass build-up is consistent with what one would predict from measurements of the SFR.
- Work on the CFHTLS Deep Fields shows that the mass in disk-dominated galaxies decreases slightly over time while the mass in bulge-dominated galaxies increases greatly over time.

**Acknowledgements.** S.D.J.G. was supported partially by a discovery grant from NSERC and from an NSERC CRO grant which supports Canadian participation in the CFHT Legacy Survey.

## References

- [1] Lilly, S. J., Fèvre, O. L., Hammer, F., & Crampton, D. 1996, *Astrophys. J. Let.*, 460, L1
- [2] Madau, P., Ferguson, H. C., Dickinson, M. E., Giavalisco, M., Steidel, C. C., & Fruchter, A. S. 1996, *M.N.R.A.S.*, 283, 1388
- [3] Madau, P., Pozzetti, L., & Dickinson, M. 1998, *Astrophys. J.*, 498, 106
- [4] Bouwens, R. J., Illingworth, G. D., Thompson, R. I., Blakeslee, J. P., Dickinson, M. E., Broadhurst, T. J., Eisenstein, D. J., Fan, X., Franx, M., Meurer, G., & van Dokkum, P. 2004a, *ApJ*, 606, L25
- [5] Bouwens, R. J., Thompson, R. I., Illingworth, G. D., Franx, M., van Dokkum, P. G., Fan, X., Dickinson, M. E., Eisenstein, D. J., & Rieke, M. J. 2004b, *ApJ*, 616, L79
- [6] Bunker, A. J., Stanway, E. R., Ellis, R. S., & McMahon, R. G. 2004, *MNRAS*, 355, 374
- [7] Stanway, E. R., Glazebrook, K., Bunker, A. J., Abraham, R. G., Hook, I., Rhoads, J., McCarthy, P. J., Boyle, B., Colless, M., Crampton, D., Couch, W., Jørgensen, I., Malhotra, S., Murowinski, R., Roth, K., Savaglio, S., & Tsvetanov, Z. 2004, *ApJ*, 604, L13

- [8] Bertin, E., & Arnouts, S. 1996, *Astron. & Astrophys. Supp.*, 117, 393
- [9] Loh, E. D., & Spillar, E. J. 1986, *Astrophys. J.*, 303, 154
- [10] Gwyn, S. D. J. 2001, PhD thesis, University of Victoria
- [11] Coleman, G. D., Wu, C.-C., & Weedman, D. W. 1980, *Astrophys. J. Supp.*, 43, 393
- [12] Kinney, A. L., Calzetti, D., Bohlin, R. C., McQuade, K., Storchi-Bergmann, T., & Schmidt, H. R. 1996, *Astrophys. J.*, 467, 38
- [13] Fioc, M., & Rocca-Volmerange, B. 1997, *Astron. & Astrophys.*, 326, 950
- [14] Calzetti, D. 1997, in *The Ultraviolet Universe at Low and High Redshift: Probing the Progress of Galaxy Evolution*, 403, astro-ph/9706121
- [15] Kroupa, P., Tout, C. A., & Gilmore, G. 1993, *MNRAS*, 262, 545
- [16] Hartwick, F. D. A. 2004, *ApJ*, 603, 108
- [17] Gwyn, S. D. J. 2005, *AJ*, accepted
- [18] Treyer, M. A., Ellis, R. S., Milliard, B., Donas, J., & Bridges, T. J. 1998, *MNRAS*, 300, 303
- [19] Hughes, D. H., Serjeant, S., Dunlop, J., Rowan-Robinson, M., Blain, A., Mann, R. G., Ivison, R., Peacock, J., Efstathiou, A., Gear, W., Oliver, S., Lawrence, A., Longair, M., Goldschmidt, P., & Jenness, T. 1998, *Nature*, 394, 241
- [20] Flores, H., Hammer, F., Thuan, T. X., Césarsky, C., Desert, F. X., Omont, A., Lilly, S. J., Eales, S., Crampton, D., & Le Fèvre, O. 1999, *Astrophys. J.*, 517, 148
- [21] Steidel, C. C., Adelberger, K. L., Giavalisco, M., Dickinson, M., & Pettini, M. 1999, *Astrophys. J.*, 519, 1
- [22] Wilson, G., Cowie, L. L., Barger, A. J., & Burke, D. J. 2002, *AJ*, 124, 1258
- [23] Giavalisco, M., Dickinson, M., Ferguson, H. C., Ravindranath, S., Kretchmer, C., Moustakas, L. A., Madau, P., Fall, S. M., Gardner, J. P., Livio, M., Papovich, C., Renzini, A., Spinrad, H., Stern, D., & Riess, A. 2004, *ApJ*, 600, L103
- [24] Rudnick, G., Rix, H., Franx, M., Labbé, I., Blanton, M., Daddi, E., Förster Schreiber, N. M., Moorwood, A., Röttgering, H., Trujillo, I., van de Wel, A., van der Werf, P., van Dokkum, P. G., & van Starkenburg, L. 2003, *ApJ*, 599, 847
- [25] Dickinson, M., Papovich, C., Ferguson, H. C., & Budavári, T. 2003, *ApJ*, 587, 25
- [26] Fontana, A., Pozzetti, L., Donnarumma, I., Renzini, A., Cimatti, A., Zamorani, G., Menci, N., Daddi, E., Giallongo, E., Mignoli, M., Perna, C., Salimbeni, S., Saracco, P., Broadhurst, T., Cristiani, S., D'Odorico, S., & Gilmozzi, R. 2004, *A&A*, 424, 23
- [27] Drory, N., Bender, R., Feulner, G., Hopp, U., Maraston, C., Snigula, J., & Hill, G. J. 2004, *ApJ*, 608, 742
- [28] Drory, N., Salvato, M., Gabasch, A., Bender, R., Hopp, U., Feulner, G., & Pannella, M. 2005, *ApJ*, 619, L131
- [29] Schade, D. and Lilly, S. J. and Le Fevre, O. and Hammer, F. & Crampton, D. 1996, *ApJ*, 464, 79
- [30] Bundy, K. and Ellis, R. S. and Conselice, C. J. 2005, *ApJ*, 625, 621